Nonlinear Dyn (2018) 92:1287–1297
https://doi.org/10.1007/s11071-018-4125-1

ORIGINAL PAPER

On the existence of periodic orbits and KAM tori in the Sprott A system: a special case of the Nosé–Hoover oscillator

Marcelo Messias · Alisson C. Reinol

Received: 13 May 2017 / Accepted: 2 February 2018 / Published online: 15 February 2018

Abstract We consider the well-known Sprott A system, which is a special case of the widely studied Nosé–Hoover oscillator. The system depends on a single real parameter a, and for suitable choices of the parameter value, it is shown to present chaotic behavior, even in the absence of an equilibrium point. In this paper, we prove that, for $a \neq 0$, the Sprott A system has neither invariant algebraic surfaces nor polynomial first integrals. For $a > 0$ small, by using the averaging method we prove the existence of a linearly stable periodic orbit, which bifurcates from a non-isolated zero-Hopf equilibrium point located at the origin. Moreover, we show numerically the existence of nested invariant tori surrounding this periodic orbit. Thus, we observe that these dynamical elements and their perturbation play an important role in the occurrence of chaotic behavior in the Sprott A system.

Keywords Sprott A system · Nosé–Hoover oscillator · Averaging method · Periodic orbits · Nested invariant tori · Invariant algebraic surfaces · Chaotic behavior

M. Messias (✉)
Departamento de Matemática e Computação, Faculdade de Ciências e Tecnologia, Universidade Estadual Paulista (UNESP), Presidente Prudente, SP, Brazil
e-mail: marcelo@fct.unesp.br

A. C. Reinol
Departamento de Matemática, Instituto de Biociências, Letras e Ciências Exatas, Universidade Estadual Paulista (UNESP), São José do Rio Preto, SP, Brazil
e-mail: alissoncarv@gmail.com

1 Introduction and statement of the main results

In the last decades, several chaotic differential systems have been reported in the literature, such as the Lorenz system [18], Chen system [5], Lü system [19], Rössler system [23] and many others. Recently, even differential systems without equilibrium points were shown to have chaotic behavior [10,13,26,30,31].

In this paper, we consider the polynomial differential system

$$\dot{x} = y, \quad \dot{y} = -x - y\,z, \quad \dot{z} = y^2 - a, \tag{1}$$

where $a \in \mathbb{R}$ and the dot denotes derivative with respect to the independent variable t, usually called *time*. In [26], Sprott presented system (1) with $a = 1$ as Case A in a list of nineteen distinct differential systems with quadratic nonlinearities and having chaotic behavior. In this way, this system is usually called *Sprott A system*. Observe that for $a = 1$ system (1) has no equilibrium points. The Sprott A system is a very important differential system in nonlinear dynamics because, beyond its theoretical importance, it has been used as source of inspiration for finding many new rare chaotic flows, see for instance [28].

From the Physical point of view, the Sprott A system is a special case of the well-known and widely studied Nosé–Hoover oscillator [8,21,22] as pointed out by Hoover in [9]. Indeed, considering, for $a > 0$, the linear change of variables

$$x = \sqrt{a}\, q, \quad y = \sqrt{a}\, p, \quad z = \xi \tag{2}$$

and taking $a = \alpha$ into system (1), it becomes equivalent to the equations used in [8,22] to describe a single one-dimensional harmonic oscillator, called Nosé–Hoover oscillator, given by

$$\dot{q} = p, \quad \dot{p} = -q - p\,\xi, \quad \dot{\xi} = \alpha\,(p^2 - 1), \tag{3}$$

where q and p are the coordinate and momentum of the oscillator, respectively, ξ is a friction coefficient, and α is a coupling positive real parameter (for details, see [22]). More recently, some generalizations of this oscillator were studied by many authors, see for instance [27] and references therein.

In [22], Posch, Hoover and Vesely developed a comprehensive analytical and numerical study of the dynamics of system (3) using standard techniques, as Lyapunov exponents and Poincaré phase space sections. In Sect. III of that work, among other facts, the authors numerically identified the existence of several types of periodic orbits as well as the existence of KAM tori in the phase space of system (3), for certain positive values of the parameter α. They also realized that, for larger values of α, both regular and chaotic solutions can be generated and the regular solutions are generally quasi-periodic and trace out KAM tori in the phase space. Indeed, in Sect. IV of [22], by studying the Poincaré sections, the authors showed that, for α sufficiently large, system (3) presents large enclosed islands of stability, consisting of regular orbits (periodic and quasi-periodic), surrounded by chaotic seas. The fractal dimension and Lyapunov instability of these chaotic regimes were also studied in [22]. As for $a \neq 0$ systems (1) and (3) are equivalent, these types of dynamics also appear in system (1), as we shall see ahead.

In the present paper, we study analytical and numerically three aspects of system (1): the nonexistence of invariant algebraic surfaces and polynomial first integrals for $a \neq 0$, which is proved using some results of Darboux theory of integrability; the existence of a (small) linearly stable periodic orbit bifurcating from the origin, for $a > 0$ sufficiently small, which is proved using the averaging method; and the existence of nested invariant tori surrounding this periodic orbit. In this way, we intend to present a more detailed study about the interesting dynamical phenomena observed in system (1) (and, consequently, of system (3)). As we are considering system (1) from a theoretical point of view, we begin our study taking $a = 0$ (as in [20]). In this case, system (1) is not equivalent to system (3), but its phase space has an interesting geometric structure, which we use as the starting point to develop our analysis.

Differential systems having chaotic behavior as system (1) usually present a very complicated dynamics and, consequently, are difficult to be studied. One of the tools used to analyze their dynamics is the determination of algebraic surfaces embedded in $\mathbb{R}^3$ which are invariant under their flow. These surfaces are called *invariant algebraic surfaces*, whose precise definition is given below.

Let $f \in \mathbb{C}[x, y, z]$ be a non-constant polynomial. The surface $f(x, y, z) = 0$ is an invariant algebraic surface of system (1) if there exists a polynomial $K \in \mathbb{C}[x, y, z]$ such that

$$\mathcal{X}(f) = P\,\frac{\partial f}{\partial x} + Q\,\frac{\partial f}{\partial y} + R\,\frac{\partial f}{\partial z} = Kf, \tag{4}$$

where $\mathcal{X} = (P, Q, R) = (y,\ -x - yz,\ y^2 - a)$ is the vector field associated with system (1). The polynomial K is called the *cofactor* of the invariant algebraic surface $f = 0$. If $K \equiv 0$, then we say that f is a *polynomial first integral* of system (1).

In [20], Messias and Reinol proved that, for $a = 0$, the phase space of the Sprott A system is foliated by the invariant spheres $x^2+y^2+z^2 = r^2$, with $r > 0$, because it has the polynomial first integral $f(x, y, z) = x^2 + y^2 + z^2$. They also showed the existence of infinitely many heteroclinic orbits of south pole–north pole type on each invariant sphere, as shown in Fig. 1. Here, we prove the following result.

Theorem 1 *If $a \neq 0$ in differential system (1), then the system has neither invariant algebraic surfaces nor polynomial first integrals.*

Theorem 1 is proved in Sect. 2. This result is also valid for system (3) with $\alpha \neq 0$, due to its equivalence with system (1) in this case.

By varying the value of parameter a in system (1), Messias and Reinol performed in [20] a detailed numerical analysis of this system when the spheres $x^2 + y^2 + z^2 = r^2$ are no longer invariant algebraic surfaces of system (1); consequently, the heteroclinic orbits are destroyed. For $a > 0$ small enough, they numerically detected the existence of nested invariant tori in a neighborhood of the origin and, for larger val-

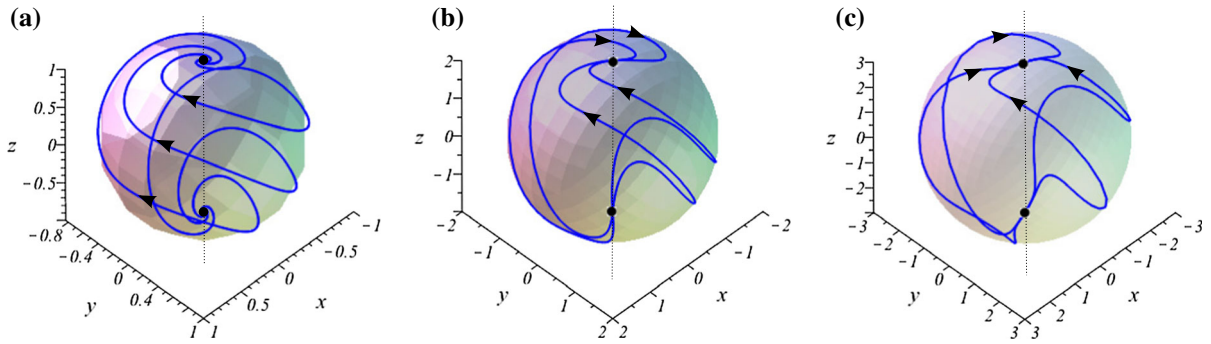

Fig. 1 Flow of system (1) with $a = 0$ restricted to the invariant spheres $x^2 + y^2 + z^2 = r^2$ for **a** $0 < r < 2$, **b** $r = 2$ and **c** $r > 2$. Note that the heteroclinic orbits on the invariant spheres connect a pair of foci in (**a**), improper nodes in (**b**) and nodes in (**c**)

ues of a, these tori are surrounded by a chaotic sea. In particular, they observed the occurrence of chaos even for $a < 1$, more precisely for $a = 0.4$ (for more details see [20]). The study developed here complements and clarifies the results presented in [20,22] and helps to better understand the interesting dynamics phenomena observed in Sprott A system.

For $a = 0$, system (1) has a line of equilibria at the z–axis and the origin is a non-isolated zero-Hopf equilibrium point. We recall that an (isolated) equilibrium point of a differential system in $\mathbb{R}^3$ is a *zero-Hopf equilibrium* if it has one zero and a pair of purely imaginary eigenvalues. As for $a = 0$ the origin of system (1) is a non-isolated equilibrium point with eigenvalues 0 and $\pm i$, we call it a non-isolated zero-Hopf equilibrium point. In [17], by using the averaging theory of second order, the authors proved the existence of one or two limit cycles bifurcating from a non-isolated zero-Hopf equilibrium point in certain families of three-dimensional differential systems.

Here, by using the averaging theory of first order we prove that, for $a > 0$ small enough, a small amplitude periodic orbit bifurcates from the origin of system (1). Moreover, by numerical simulations, we show the existence of nested invariant tori surrounding this periodic orbit, as shown in Fig. 2. More precisely, the following result holds.

Theorem 2 *For $a > 0$ small enough, there exists a linearly stable periodic orbit in the phase space of system (1), which tends to the origin as $a \to 0$ and it is surrounded by nested invariant tori.*

Theorem 2 is proved in Sect. 4. From Theorem 1, it follows that the invariant tori surrounding the periodic orbit are not algebraic surfaces. Also, the periodic orbit and the nested invariant tori described in Theorem 2 are very small, as can be seen in Fig. 2. Indeed, they bifurcate from the origin when the parameter value is varied from $a = 0$ to $a > 0$ small; on the other hand, they shrink into the origin as $a \to 0$. In this way, the periodic orbit and the invariant tori of Sprott A system are much smaller than the periodic orbits and invariant tori of system (3), presented in Figs. 1 to 7 of [22]. It happens because the geometric structure of the phase space of Nosé–Hoover oscillator (3) with $\alpha = 0$ is quite different from the geometric structure of the Sprott A system with $a = 0$, described above (for more details, see [20]). In fact, for $\alpha = 0$ system (3) has the invariant planes $\xi = c \in \mathbb{R}$, on which the dynamics are given by the following planar system

$$\dot{q} = p, \quad \dot{p} = -q - p\,c.$$

Observe that, on the plane $\xi = c = 0$, the origin is a center. It can be shown that, for $\alpha > 0$ small, a periodic orbit bifurcates from the circle $x^2 + y^2 = 2$ belonging to this invariant plane (see [14]). Hence, the periodic orbit of system (3) which exist for α small is "big", compared to the periodic orbit of the Sprott A system with small a. The difference in the scales of periodic orbits and invariant tori of systems (1) and (3) are due to the linear change of variables (2), which gives the equivalence between these systems. Therefore, the change in scale must be taken into account when comparing the dynamics of Sprott A system and Nosé–Hoover oscillator.

It is known that, generically, a *zero-Hopf (or fold-Hopf) bifurcation* takes place in an isolated zero-Hopf equilibrium point of a two-parameter family of three-

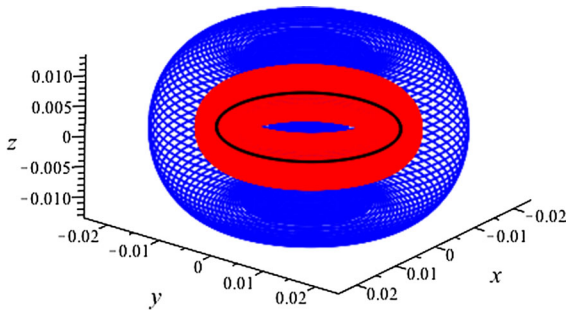

Fig. 2 Nested invariant tori surrounding the periodic orbit of system (1) for $a = 10^{-4}$

dimensional differential systems. In a small neighborhood of this type of equilibrium point, the unfolding can exhibit different topological types of dynamics, as the two parameters vary. Depending on the system, even a branch of torus bifurcations (Neimark-Sacker bifurcation) can emanate from the zero-Hopf equilibrium point and, in some cases, the zero-Hopf bifurcation can imply a local birth of chaos, as stated for instance in [1,2,25]. For more details about this type of bifurcation, see [6,7,12,25]. System (1) depends on a single real parameter a and, for $a = 0$, the origin is a non-isolated zero-Hopf equilibrium point. Hence, it cannot exhibit a complete unfolding of a classical zero-Hopf bifurcation. Therefore, the bifurcation that occurs in the origin of Sprott A system as the parameter a is varied is one of the possible bifurcations which can occur in the complete unfolding of such a degenerate equilibrium point. In particular, it is different from the bifurcations described in [17] for a non-isolated zero-Hopf equilibrium point.

We observe that the chaotic seas described in [20] and in [22] arises due to the destruction of some invariant tori surrounding the periodic orbit, as the parameter a is varied. Hence, the emergence of a periodic orbit from the origin and the existence of nested invariant tori around it play an important role in the occurrence of chaotic behavior in system (1).

This paper is devoted to prove Theorems 1 and 2, and it is organized as follows. In Sect. 2, we prove Theorem 1. In Sect. 3, we present some basic aspects of the averaging theory, which will be used in Sect. 4 to prove Theorem 2. Some concluding remarks are given in Sect. 5. Furthermore, some numerical results are provided along the text, in order to study the chaotic behavior of system (1), to corroborate the analytical results obtained and to show the existence of KAM tori.

2 Proof of Theorem 1

Consider $a \neq 0$ in system (1). Suppose that $f = 0$ is an invariant algebraic surface of degree $n \geq 1$ of this system with cofactor $K = k_0 + k_1 x + k_2 y + k_3 z$, with $k_0, k_1, k_2, k_3 \in \mathbb{C}$. Assume that K is not identically zero. Take f as the sum of its homogeneous parts, that is $f = \sum_{i=0}^{n} f_i$, where each f_i is a homogeneous polynomial of degree i, for $i = 0, \ldots, n$. Assume that $n > 1$ (we can easily verify that system (1) has no invariant planes). From the definition of invariant algebraic surface, f must satisfy equality (4), that is

$$y \frac{\partial f}{\partial x} + (-x - y z) \frac{\partial f}{\partial y} + (y^2 - a) \frac{\partial f}{\partial z} = (k_0 + k_1 x + k_2 y + k_3 z) f. \tag{5}$$

Computing the terms of degree $n+1$ in (5), we obtain

$$- y z \frac{\partial f_n}{\partial y} + y^2 \frac{\partial f_n}{\partial z} = (k_1 x + k_2 y + k_3 z) f_n. \tag{6}$$

Solving this partial differential equation, we get

$$f_n(x, y, z) = C_n(x, y^2 + z^2) \times \left(\frac{2y^2 + 2z^2 + 2z\sqrt{y^2 + z^2}}{y} \right)^{g(x,y,z)} \times \exp\left(- k_2 \arctan\left(\frac{y}{z} \right) \right) y^{-k_3},$$

where C_n is an arbitrary function in the variables x and $y^2 + z^2$ and $g(x, y, z) = k_1 x / \sqrt{y^2 + z^2}$. As f_n is a homogeneous polynomial of degree n, we must have $k_1 = k_2 = 0$ and $k_3 = -m$, with $0 \leq m \leq n$ an integer. Hence, $f_n(x, y, z) = C_n(x, y^2 + z^2)\, y^m$.

Now, computing the terms of degree n in (5), we obtain

$$- y z \frac{\partial f_{n-1}}{\partial y} + y^2 \frac{\partial f_{n-1}}{\partial z} + y \frac{\partial f_n}{\partial x} - x \frac{\partial f_n}{\partial y} = k_0 f_n - m z f_{n-1}. \tag{7}$$

We consider two cases: $m = 0$ and $m \neq 0$. Assuming that $m = 0$ in (7) and solving this partial differential equation for f_{n-1}, we get

$$f_{n-1}(x, y, z) = C_{n-1}(x, y^2 + z^2) + \frac{\partial f_n}{\partial x} \arctan\left(\frac{y}{z} \right) + h(y, z) \left(x \frac{\partial f_n}{\partial y} + k_0 f_n \right),$$

where C_{n-1} is an arbitrary function in the variables x and y^2+z^2, and

$$h(y,z)=\frac{1}{\sqrt{y^2+z^2}}\ln\left(\frac{2y^2+2z^2+2z\sqrt{y^2+z^2}}{y}\right). \tag{8}$$

Since f_{n-1} is a homogeneous polynomial of degree $n-1$, we must have

$$x\,\frac{\partial f_n}{\partial y}+k_0\,f_n=0,$$

whose solution is

$$f_n(x,y,z)=C_n(x,z)\,\exp\left(-\frac{k_0\,y}{x}\right),$$

where C_n is an arbitrary function in the variables x and z. Hence, $k_0=0$, because f_n is a homogeneous polynomial. Thus, $K\equiv 0$, what is a contradiction, since we are considering K not identically zero.

Now, consider $m\neq 0$ in the partial differential equation (7). Without loss of generality, we can assume that $m=1$. Solving the partial differential equation for f_{n-1}, we get

$$f_{n-1}(x,y,z)=C_{n-1}(x,y^2+z^2)\,y-h(y,z)\,y\,\frac{\partial f_n}{\partial x}+\frac{z}{y^2+z^2}\left(x\,\frac{\partial f_n}{\partial y}+k_0\,f_n\right),$$

where C_{n-1} is an arbitrary function in the variables x and y^2+z^2, and $h(y,z)$ is given by (8). Since f_{n-1} is a homogeneous polynomial, we must have

$$x\,\frac{\partial f_n}{\partial y}+k_0\,f_n=F(x,y,z)\,(y^2+z^2),$$

where F is an arbitrary polynomial. The solution of this partial differential equation is

$$f_n(x,y,z)=C_n(x,z)\,\exp\left(-\frac{k_0\,y}{x}\right)+F(x,y,z)\,\frac{k_0^2\,(y^2+z^2)+2\,x^2-2\,k_0\,x\,y}{k_0^3},$$

where C_n is an arbitrary function in the variables x and z. Note that, in this case, f_n is not a polynomial for $k_0\neq 0$. Consider $F(x,y,z)=k_0^3\,\tilde{F}(x,y,z)$, where $\tilde{F}$ is an arbitrary polynomial. Then, taking $k_0=0$, we obtain that $f_n=C_n(x,z)$. As we also have that $f_n(x,y,z)=C_n(x,y^2+z^2)\,y^m$ (solution of the partial differential equation (6)) and we are considering $m\neq 0$, it follows that $f_n\equiv 0$, which is a contradiction, because by hypothesis f is a polynomial of degree n. Therefore, for $a\neq 0$, system (1) has no invariant algebraic surfaces.

Now, suppose that the cofactor K is identically zero, that is f is a polynomial first integral of system (1). Then, f satisfies equality (5) with $k_0=k_1=k_2=k_3=0$. In this case, computing the terms of degree n in (5), we obtain

$$-y\,z\,\frac{\partial f_{n-1}}{\partial y}+y^2\,\frac{\partial f_{n-1}}{\partial z}+y\,\frac{\partial f_n}{\partial x}-x\,\frac{\partial f_n}{\partial y}=0.$$

Solving this partial differential equation for f_{n-1}, we obtain

$$f_{n-1}=C_{n-1}(x,y^2+z^2)+\frac{\partial f_n}{\partial x}\arctan\left(\frac{y}{z}\right)+h(y,z)\,x\,\frac{\partial f_n}{\partial y},$$

where C_{n-1} is an arbitrary function in the variables x and y^2+z^2, and $h(y,z)$ is given by (8). As f_{n-1} is a homogeneous polynomial, we must have $\partial f_n/\partial x\equiv\partial f_n/\partial y\equiv 0$. Hence, $f_n(x,y,z)=c\,z^n$, with $c\in\mathbb{C}$, because f_n is a homogeneous polynomial of degree n which only depends on the variable z. Now, computing the terms of degree $n-1$ in (5), with $k_0=k_1=k_2=k_3=0$, we obtain

$$-y\,z\,\frac{\partial f_{n-2}}{\partial y}+y^2\,\frac{\partial f_{n-2}}{\partial z}+y\,\frac{\partial f_{n-1}}{\partial x}-x\,\frac{\partial f_{n-1}}{\partial y}-\frac{\partial f_n}{\partial z}\,a=0.$$

Solving this partial differential equation for f_{n-2}, we get

$$f_{n-2}(x,y,z)=C_{n-2}(x,y^2+z^2)+\frac{\partial f_{n-1}}{\partial x}\arctan\left(\frac{y}{z}\right)+h(y,z)\left(x\,\frac{\partial f_{n-1}}{\partial y}+a\,\frac{\partial f_n}{\partial z}\right),$$

where C_{n-2} is an arbitrary function in the variables x and y^2+z^2, and $h(y,z)$ is given by (8). Since f_{n-2} is a homogeneous polynomial and remembering that $f_n(x,y,z)=c\,z^n$, we must solve the partial differential equation

$$x\,\frac{\partial f_{n-1}}{\partial y}+a\,c\,n\,z^{n-1}=0,$$

whose solution is

$$f_{n-1}(x,y,z)=C_{n-1}(x,z)-a\,c\,n\,\frac{y\,z^{n-1}}{x}.$$

Since f_{n-1} is a homogeneous polynomial, $a \neq 0$ (by hypothesis) and $n > 1$, we must have $c = 0$ and, consequently, $f_n \equiv 0$, what is a contradiction, because f is a polynomial of degree n. Therefore, for $a \neq 0$, system (1) has no polynomial first integrals. This ends the proof of Theorem 1. □

3 Averaging theory of first order

In this section, we give a result from the averaging theory, which will be used to prove the existence of the periodic orbit stated in Theorem 2. A nice introduction to this theory can be found in [24], while recent works which extend and improve it are given in [3,4,15,16].

Consider the initial value problems

$$\dot{\mathbf{x}} = \varepsilon\, F_1(t, \mathbf{x}) + \varepsilon^2\, F_2(t, \mathbf{x}, \varepsilon), \quad \mathbf{x}(0) = \mathbf{x}_0, \tag{9}$$

and

$$\dot{\mathbf{y}} = \varepsilon\, g(\mathbf{y}), \quad \mathbf{y}(0) = \mathbf{x}_0, \tag{10}$$

with $\mathbf{x}$, $\mathbf{y}$ and $\mathbf{x}_0$ in some open subset Ω of $\mathbb{R}^n$, $t \in [0, \infty)$ and $\varepsilon \in (0, \varepsilon_0]$, for some fixed $\varepsilon_0 > 0$ sufficiently small. Assume that F_1 and F_2 are periodic functions of period T in the variable t, and set

$$g(\mathbf{y}) = \frac{1}{T} \int_0^T F_1(t, \mathbf{y}) dt.$$

Denote by $D_{\mathbf{x}} g$ all the first derivatives of g and by $D_{\mathbf{xx}} g$ all the second derivatives of g. Under these assumptions, the following result holds.

Theorem 3 *Assume that F_1, $D_{\mathbf{x}} F_1$, $D_{\mathbf{xx}} F_1$ and $D_{\mathbf{x}} F_2$ are continuous and bounded by a constant independent of ε in $[0, \infty) \times \Omega \times (0, \varepsilon_0]$, and that $\mathbf{y}(t) \in \Omega$ for $t \in [0, 1/\varepsilon]$. Then, the following statements hold.*

1. *For $t \in [0, 1/\varepsilon]$, we have $\mathbf{x}(t) - \mathbf{y}(t) = \mathcal{O}(\varepsilon)$ as $\varepsilon \to 0$.*
2. *If $p \neq 0$ is an equilibrium point of system (10) such that $\det[D_{\mathbf{y}} g(p)] \neq 0$, then there exists a periodic solution $\phi(t, \varepsilon)$ of period T for system (9) which is close to p and such that $\phi(0, \varepsilon) - p = \mathcal{O}(\varepsilon)$ as $\varepsilon \to 0$.*
3. *The stability of the periodic solution $\phi(t, \varepsilon)$ is given by the stability of the equilibrium point p.*

For a proof of Theorem 3, see [6,29].

4 Proof of Theorem 2

In this section, we use Theorems 3 to prove Theorem 2.

Proof of Theorem 2 Before applying Theorem 3 in differential system (1), we need to write its linear part at the origin into the real Jordan normal form. After a rescaling of the time t, system (1) can be written as

$$\dot{x} = -y, \quad \dot{y} = x + y\, z, \quad \dot{z} = -y^2 + a. \tag{11}$$

Now, writing system (11) in cylindrical coordinates (r, θ, z), where $x = r\, \cos\theta$, $y = r\, \sin\theta$, it becomes

$$\begin{aligned} \dot{r} &= r\, z\, \sin^2\theta, \\ \dot{\theta} &= z\, \sin\theta\, \cos\theta + 1, \\ \dot{z} &= a - r^2\, \sin^2\theta. \end{aligned} \tag{12}$$

Considering the change of variables $r = \varepsilon\, R$, $z = \varepsilon\, Z$, with $\varepsilon = \sqrt{a} > 0$, system (12) can be written as

$$\begin{aligned} \dot{R} &= \varepsilon\, R\, Z\, \sin^2\theta, \\ \dot{\theta} &= \varepsilon\, Z\, \sin\theta\, \cos\theta + 1, \\ \dot{Z} &= \varepsilon\, (1 - R^2\, \sin^2\theta). \end{aligned}$$

Taking θ as the independent variable and doing the Taylor expansion of order 2 of the obtained equations at $\varepsilon = 0$, we get

$$\begin{aligned} \frac{dR}{d\theta} &= \varepsilon\, R\, Z\, \sin^2\theta + \mathcal{O}(\varepsilon^2), \\ \frac{dZ}{d\theta} &= (1 - R^2\, \sin^2\theta)\, \varepsilon + \mathcal{O}(\varepsilon^2). \end{aligned} \tag{13}$$

Using the notation of Theorem 3, consider

$$\begin{aligned} &\mathbf{x} = \begin{pmatrix} R \\ Z \end{pmatrix}, \\ &t = \theta, \\ &T = 2\pi, \\ &F_1(\theta, \mathbf{x}) = \begin{pmatrix} R\, Z\, \sin^2\theta \\ 1 - R^2 \sin^2\theta \end{pmatrix}. \end{aligned}$$

In this way,

$$g(\mathbf{y}) = \frac{1}{2\pi} \int_0^{2\pi} F_1(\theta, \mathbf{y})\, d\theta = \begin{pmatrix} \frac{1}{2} R\, Z \\ 1 - \frac{1}{2} R^2 \end{pmatrix}.$$

We have that $g(\mathbf{y}) = 0$ has the unique real solution $p = (R, Z) = (\sqrt{2}, 0)$ (remember that $R > 0$), which satisfies $\det[D_{\mathbf{y}} g(p)] = 1 \neq 0$. Then, by Theorem 3, it

follows that, for $\varepsilon > 0$ sufficiently small, system (13) has a periodic solution $\phi(\theta, \varepsilon) = (R(\theta, \varepsilon), Z(\theta, \varepsilon))$ such that $\phi(0, \varepsilon) \to (\sqrt{2}, 0)$ as $\varepsilon \to 0$. Moreover, the eigenvalues of the matrix $[D_{\mathbf{y}} g(p)]$ are $\pm i$. Hence, the obtained periodic solution is linearly stable, that is, any solution close enough to this periodic solution remains close enough forever, without tending to it.

Going back to differential system (1), we get that, for $a > 0$ sufficiently small, such system has a periodic solution of period approximately 2π given by

$$x(t) = \sqrt{2a}\,\cos t + \mathcal{O}(a),$$
$$y(t) = -\sqrt{2a}\,\sin t + \mathcal{O}(a),$$
$$z(t) = \mathcal{O}(a).$$

Note that this solution tends to the origin as $a \to 0$. Therefore, for $a > 0$ sufficiently small system (1) has a linearly stable periodic orbit which emerges from the origin. In Fig. 3 is drawn the periodic orbit of system (1) for $a > 0$ small.

As the obtained periodic orbit is linearly stable, orbits sufficiently close to it remain near of the periodic

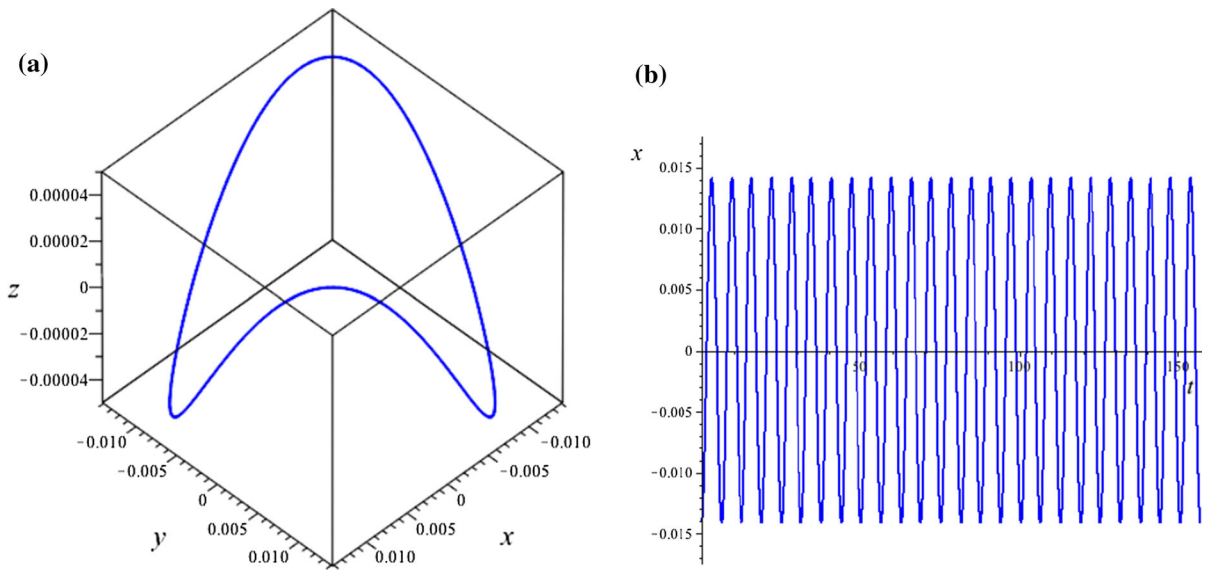

Fig. 3 **a** Periodic orbit of system (1) near of the origin for $a = 10^{-4}$ and **b** its x-coordinate in function of the time t

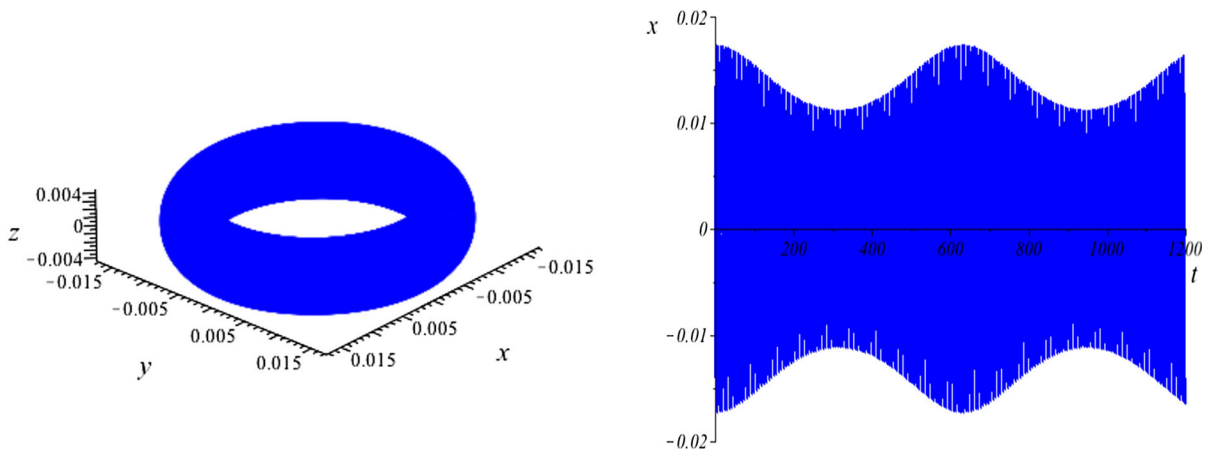

Fig. 4 **a** An orbit of system (1) with initial condition on one of the invariant tori and **b** its x-coordinate in function of the time t. The orbit is dense and moves quasi-periodically on the invariant torus. Here, $a = 10^{-4}$

orbit without tending to it. In this way, studying numerically the dynamics of system (1) in a neighborhood of the periodic orbit we observe the existence of nested invariant tori. In Fig. 4 is drawn an orbit of system (1) for $a = 10^{-4}$ with initial condition on one of these invariant tori. This fact is corroborated by the Poincaré sections in Fig. 6a–c, a central fixed point (representing the periodic orbit) is surrounded by concentric closed curves (nested invariant tori). Moreover, yet by numerical simulations, we note that orbits are dense and move quasi-periodically on these tori. □

The existence of nested invariant tori was also observed in [20,22], and in the last one authors called them KAM tori.

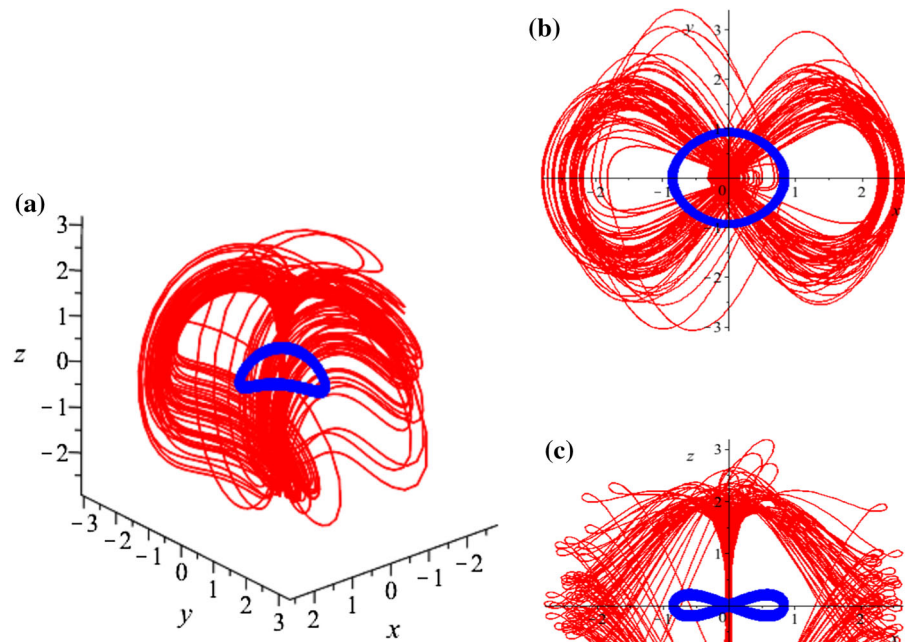

Fig. 5 **a** Orbits of system (1) with initial condition on an invariant torus (blue) and in the chaotic sea (red) and their projections **b** on the xy-plane and **c** on the xz-plane. Parameter value: $a = 10^{-4}$. (Color figure online)

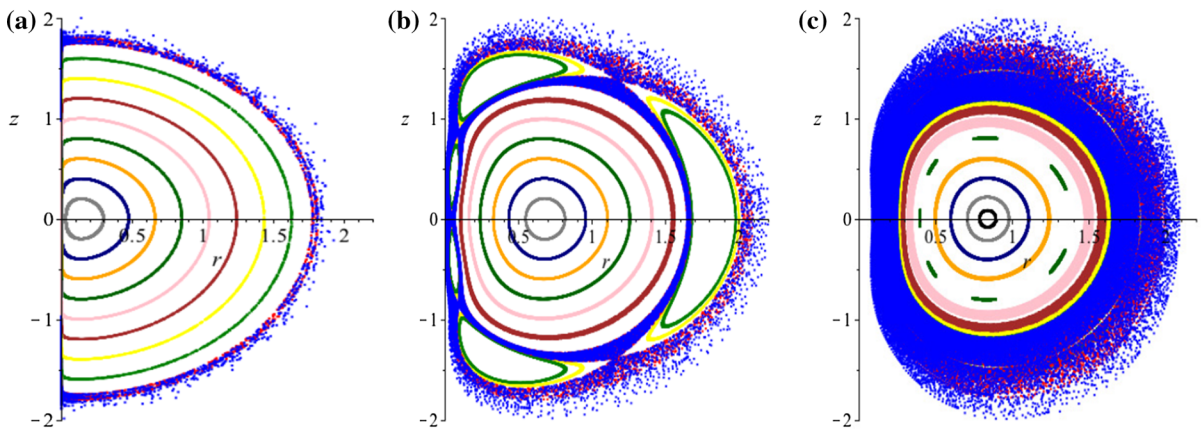

Fig. 6 Poincaré section of system (1) in a neighborhood of the periodic orbit for **a** $a = 0.01$, **b** $a = 0.25$ and **c** $a = 0.4$. In cases (**a**)–(**c**), we consider the same initial conditions, which are represented in different colors. (Color figure online)

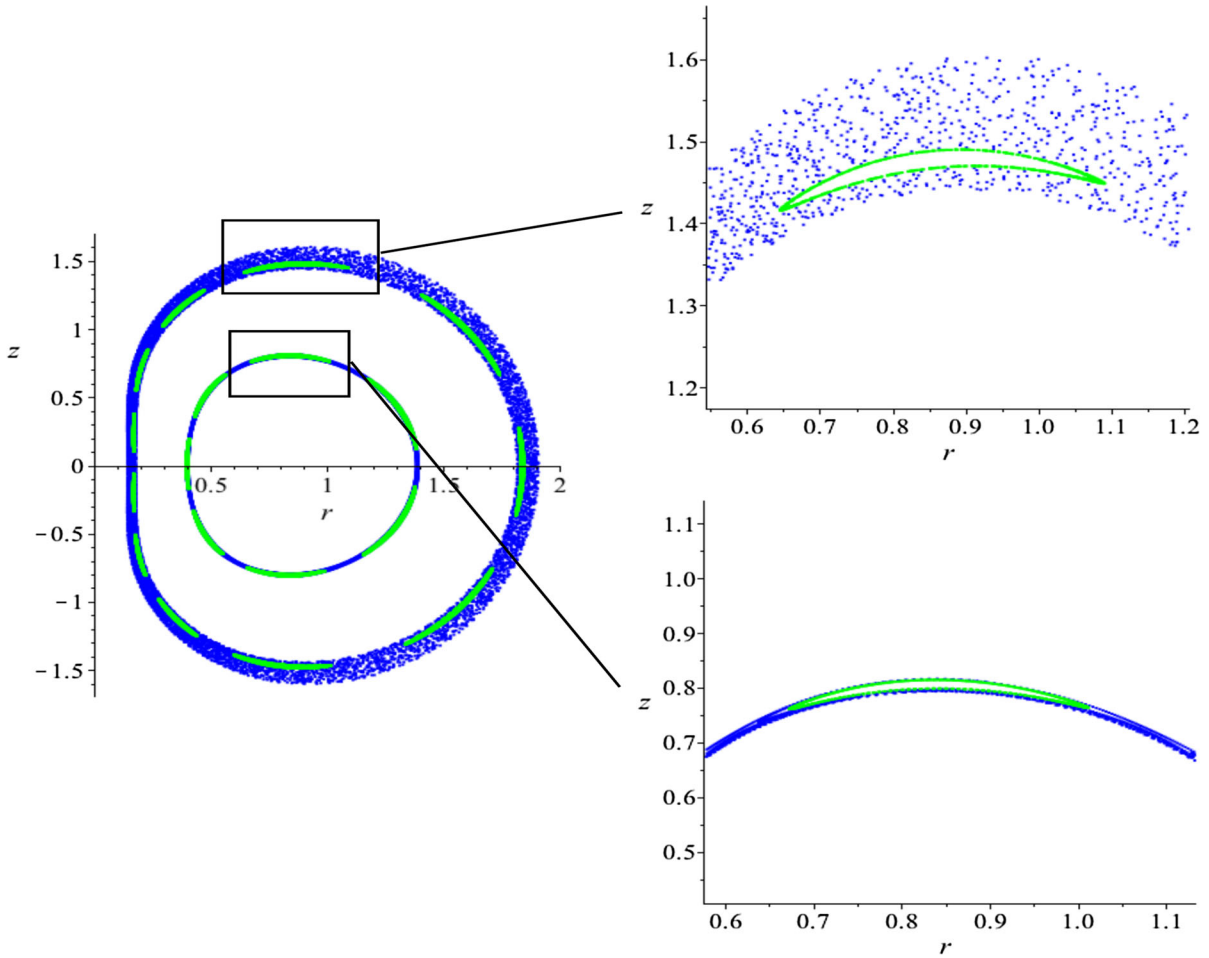

Fig. 7 Regular islands in the Poincaré section of system (1) for $a = 0.4$ (Fig. 6c)

4.1 Chaotic behavior

For suitable values of the parameter $a > 0$, it is possible to detect chaotic behavior in system (1) (see [20,26]). In these cases, there is a chaotic sea coexisting with the nested invariant tori described in Theorem 2. In Fig. 5 are drawn in red one orbit passing by the chaotic sea and in blue one orbit belonging to one of the invariant tori of system (1), for $a = 0.4$. The coexistence of chaotic seas and invariant tori in the Sprott A system was also observed in [11] for $a = 1$ and in [22] for the equivalent Nosé–Hoover oscillator for certain values of the parameter α.

In Fig. 6 is drawn the Poincaré section of system (1) in a neighborhood of the periodic orbit for different parameters values, that is, $a = 0.01$, $a = 0.25$ and $a = 0.4$. The numerical simulations shown in Fig. 6 confirm the existence of nested invariant tori (represented by the closed curves) around the periodic orbit (represented by the central fixed point surrounded by these closed curves). Encompassing the most external invariant torus in that figure, we can see a "turbulent" region which becomes chaotic for suitable choices of the parameter. Indeed, for $a = 0.25$ (Fig. 6b) it is easy to see some chaotic seas surrounding islands of regular motions, formed by periodic and quasi-periodic orbits on the invariant tori, which indicate the complicated dynamics of system (1) and provide strong evidences of chaotic behavior. This can also be observed, although less evidently, for $a = 0.4$ (Fig. 6c). For a better viewing of such islands in this case, see Fig. 7.

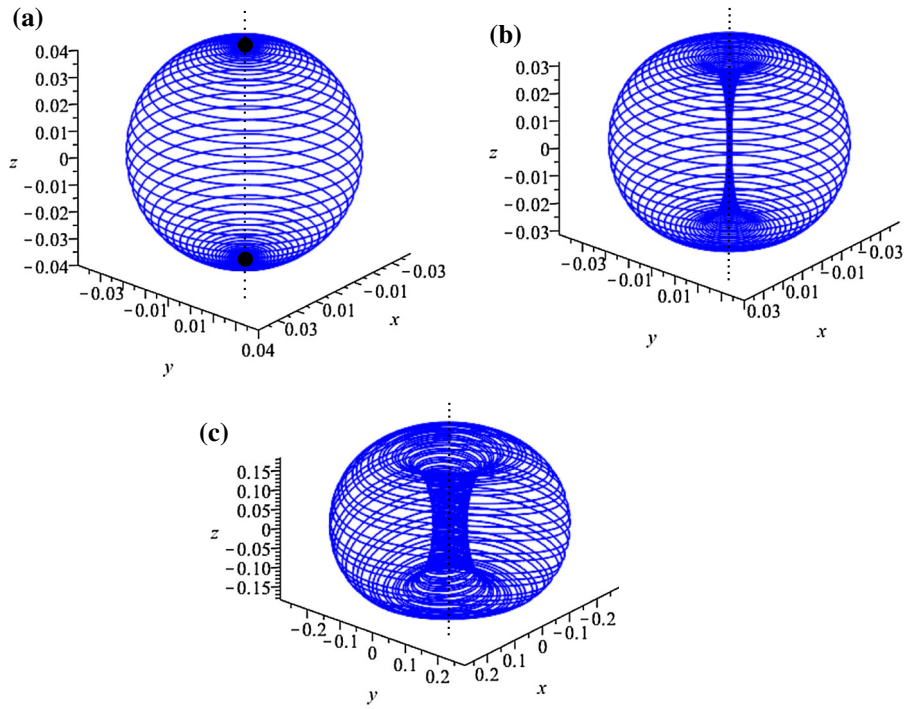

Fig. 8 Orbit with initial condition (0, 0.04, 0) for **a** $a = 0$, **b** $a = 10^{-4}$ and **c** $a = 10^{-2}$. The invariant sphere (**a**) evolves into an invariant torus (**b**) which persists for small variations of the value of parameter a (**c**)

5 Concluding remarks

In this paper, we prove that, for $a \neq 0$, the Sprott A system, which is a special case of the Nosé–Hoover oscillator, has neither invariant algebraic surfaces nor polynomial first integrals. For $a > 0$ small, there exist a linearly stable periodic orbit, which emerges from a non-isolated zero-Hopf equilibrium point located at the origin, and nested invariant tori around this periodic orbit. The results obtained here confirm what is stated in [29]: around a linearly stable periodic orbit, there are tori on which the orbits move quasi-periodically. Therefore, in synthesis, the concentric invariant spheres which exist for the Sprott A system when $a = 0$ (see [20]) evolve into nested invariant tori for $a > 0$ sufficiently small (see Fig. 8). Note that from Theorem 1, these tori are not invariant algebraic surfaces. For suitable choices of the parameter value a, it is possible to detect chaotic behavior in system (1) [20,26], which is corroborated by the Poincaré sections in Fig. 6a–c, where we can observe chaotic seas coexisting with islands of regular motion. The same type of results was numerically obtained in [22] for the Nosé–Hoover harmonic oscillator, as pointed out along the text. We can conclude that the existence of a periodic orbit bifurcating from the origin and nested invariant tori around it consists of basic dynamical elements which lead to the occurrence of chaotic behavior in the Sprott A system as well as in the Nosé–Hoover oscillator.

Acknowledgements The first author is supported by FAPESP Grant Number 2013/24541–0, by CNPq Grant Number 308159/2015–2 and by CAPES - Program CSF-PVE, Grant Number 88881.030454/2013. The second author is supported by FAPESP Grant Number 2013/26602-7. They are also grateful to the anonymous referee who pointed out the equivalence between the Sprott A system and the Nosé–Hoover oscillator, which enabled them to enrich the presentation of the results in this paper, by comparing both systems.

References

1. Baldomá, I., Seara, T.M.: Brakdown of heteroclinic orbits for some analytic unfoldings of the Hopf-zero singularity. J. Nonlinear Sci. **16**, 543–582 (2006)
2. Broer, H.W., Vegter, G.: Subordinate Sil'nikov bifurcations near some singularities of vector fields having low codimension. Ergod. Theory Dyn. Syst. **4**, 509–525 (1984)
3. Buică, A., Giné, J., Llibre, J.: A second order analysis of the periodic solutions for nonlinear periodic differential systems with a small parameter. Phys. D **241**, 528–533 (2012)
4. Cândido, M.R., Llibre, J., Novaes, D.D.: Persistence of periodic solutions for higher order perturbed differential systems via Lyapunov–Schmidt reduction. Nonlinearity **30**, 3560–3586 (2017)

5. Chen, G., Ueta, T.: Yet another chaotic attractor. Int. J. Bifurcat. Chaos **9**, 1465–1466 (1999)
6. Guckenheimer, J., Holmes, P.: Nonlinear Oscillations, Dynamical Systems and Bifurcations of Vector Fields. Springer-Verlag, New York (2002)
7. Han, M.: Existence of periodic orbits and invariant tori in codimension two bifurcations of three-dimensional systems. J. Syst. Sci. Math. Sci. **18**, 403–409 (1998)
8. Hoover, W.G.: Canonical dynamics: equilibrium phase-space distributions. Phys. Rev. A **31**, 1695–1697 (1985)
9. Hoover, W.G.: Remark on 'Some simple chaotic flows'. Phys. Rev. E **51**, 759–760 (1995)
10. Jafari, S., Sprott, J.C., Golpayegani, S.M.R.H.: Elementary quadratic chaotic flows with no equilibria. Phys. Lett. A **377**, 699–702 (2013)
11. Jafari, S., Sprott, J.C., Nazarimehr, F.: Recent new examples of hidden attractors. Eur. Phys. J. Special Top. **224**, 1469–1476 (2015)
12. Kuznetsov, YuA: Elements of Applied Bifurcation Theory. Springer, New York (2004)
13. Li, C., Sprott, J.C.: Coexisting hidden attractors in a 4-D simplified Lorenz system. Int. J. Bifurcat. Chaos **24**, 1450034 (2014). (12 pages)
14. Llibre, J., Messias, M.: Global dynamics of the Nosé–Hoover oscillator: existence of periodic orbits and formation of invariant tori. Preprint (2017)
15. Llibre, J., Novaes, D.D.: Improving the averaging theory for computing periodic solutions of the differential equations. Z. Angew. Math. Phys. **66**, 1401–1412 (2015)
16. Llibre, J., Novaes, D.D., Teixeira, M.A.: Higher order averaging theory for finding periodic solutions via Brouwer degree. Nonlinearity **27**, 563–583 (2014)
17. Llibre, J., Xiao, D.: Limit cycles bifurcating from a non-isolated zero-Hopf equilibrium of three-dimensional differential systems. Proc. Am. Math. Soc. **142**, 2047–2062 (2014)
18. Lorenz, E.N.: Deterministic nonperiodic flow. J. Atmos. Sci. **20**, 130–141 (1963)
19. Lü, J.H., Chen, G.R.: A new chaotic attractor coined. Int. J. Bifurcat. Chaos **12**, 659–661 (2002)
20. Messias, M., Reinol, A.C.: On the formation of hidden chaotic attractors and nested invariant tori in the Sprott A system. Nonlinear Dyn. **88**, 807–821 (2017)
21. Nosé, S.: A unified formulation of the constant temperature molecular-dynamics methods. J. Chem. Phys. **81**, 511–519 (1984)
22. Posch, H.A., Hoover, W.G., Vesely, F.J.: Canonical dynamics of the Nosé oscillator: stability, order, and chaos. Phys. Rev. A **33**, 4253–4265 (1986)
23. Rössler, O.: An equation for continuous chaos. Phys. Lett. A **57**, 397–398 (1976)
24. Sanders, J.A., Verhulst, F., Murdock, J.: Averaging Methods in Nonlinear Dynamical Systems. Springer, New York (2007)
25. Scheurle, J., Marsden, J.: Bifurcation to quasi-periodic tori in the interaction of steady state and Hopf bifurcations. SIAM J. Math. Anal. **15**, 1055–1074 (1984)
26. Sprott, J.C.: Some simple chaotic flows. Phys. Rev. E **50**, R647–R650 (1994)
27. Sprott, J.C., Hoover, W.G., Hoover, C.G.: Heat conduction, and the lack thereof, in time-reversible dynamical systems: generalized Nosé-Hoover oscillators with a temperature gradient. Phys. Rev. E **89**, 042914 (2014)
28. Sprott, J.C., Jafari, S., Pham, V.-T., Hosseini, Z.S.: A chaotic system with a single unstable node. Phys. Lett. A **379**, 2030–2036 (2015)
29. Verhulst, F.: Nonlinear Differential Equations and Dynamical Systems. Springer-Verlag, Berlin (1996)
30. Wang, X., Chen, G.: Constructing a chaotic system with any number of equilibria. Nonlinear Dyn. **71**, 429–436 (2013)
31. Wang, Z., Cang, S., Ochola, E.O., Sun, Y.: A hyperchaotic system without equilibrium. Nonlinear Dyn. **69**, 531–537 (2012)